Fission studies with 140 MeV α particles

A. Buttkewitz,[1] H. H. Duhm,[1] F. Goldenbaum,[2] H. Machner,[2,3,*] and W. Strauß[1]
[1]*I. Institut für Experimentalphysik, Universität Hamburg, Hamburg, Germany*
[2]*Institut für Kernphysik, Forschungszentrum Jülich, Jülich, Germany*
[3]*Fachbereich Physik, Universität Duisburg-Essen, Duisburg, Germany*
(Received 23 July 2009; published 23 September 2009)

Binary fission induced by 140 MeV α particles has been measured for ^{nat}Ag, ^{139}La, ^{165}Ho, and ^{197}Au targets. The measured quantities are the total kinetic energies, fragment masses, and fission cross sections. The results are compared with other data and systematics. A minimum of the fission probability in the vicinity $Z^2/A = 24$ is observed.

DOI: 10.1103/PhysRevC.80.037603 PACS number(s): 24.75.+i, 25.85.Ge

The binary fission process in heavy elements has been systematically studied with energetic probes such as photons, protons, α particles, as well as with heavy ions. The details of such experiments can be found in Refs. [1] and [2]. Less is known about the fission of lighter nuclei and higher energies where such nuclei can fission. If the angular momentum is high then the fission barrier is reduced and even light systems like ^{60}Zn can undergo fission [3]. Here we will concentrate on reactions induced by light charged particles and in particular α particles. The low mass region is interesting since it is predicted that for a fissility parameter Z^2/A below 20 the system tends to become asymmetric. This is the so-called Businaro-Gallone point [4]. Nix and Sassi [5] found in calculations employing the liquid drop model that the probability for fission had a minimum at the quoted fissility parameter. Such a minimum corresponds of course to a maximum in the height of the fission barrier.

In the present work we extend upward the energy of α particles in order to have higher partial waves involved in the reaction. In this way one might expect to be more sensitive to the predicted asymmetric instability.

The experiments were performed at the Jülich cyclotron. A beam of α particles was focused onto the fissile targets in the center of a scattering chamber which was 1 m in diameter. The beam was then dumped into a well shielded Faraday cup. The targets were ^{nat}Ag, ^{139}La, ^{165}Ho, and ^{197}Au with thicknesses of 50 μg/cm^2, 120 μg/cm^2, 97 μg/cm^2, and 130 μg/cm^2, respectively. The rare earth targets had backings of carbon with thicknesses of 10 μg/cm^2 (La) and 30 μg/cm^2 (Ho). The lanthanum target had in addition a 30 μg/cm^2 carbon coating to avoid oxidation.

Two different setups were used in the experiments. First, two solid state detectors of 30 mm diameter, cooled to -20°, were mounted symmetrically left and right of the beam direction at angles corresponding to full momentum transfer to the compound nucleus. The solid angles were defined by collimators of 25 mm diameter. Whilst the right detector was only 57 mm away from the target the left one was at a distance of 150 mm. Thus, if a fragment was detected in the smaller solid angle, its complementary fragment should always be detected in the larger solid angle. Coincidence circuits ensured that the two fragments were from the same reaction event. A high voltage of 10 kV applied to the target holder prevented electrons from reaching the detectors.

The detectors were calibrated with fission fragments from a ^{252}Cf source applying the method of Schmitt *et al.* [6] and Kaufmann *et al.* [7]. The calibrations were performed before the experiments and at regular intervals. The energies were calculated according to the method given in Ref. [7]. The masses were estimated from $M_l = A_{CN}E_l/(E_l + E_r)$, with A_{CN} being the mass of the fissioning nucleus and similarly for M_r.

While for the heavier targets it is rather simple to distinguish between fission fragments and background, this is not so for silver. For this target we therefore performed experiments with a different setup. Again to the right of the beam was a solid state detector. To the left we employed an ionization chamber, where the anode was subdivided to allow for $\Delta E - E$ measurements. Because of a Frisch grid, the signals were independent of the position of the ionization. Position measurements were performed using a proportional counter tube situated behind a slit in the anode. The position was calibrated with a movable slit between the ionization chamber and californium source. Energy calibration was performed as before, but corrections had to be applied for the entrance window of the ionization chamber.

Backgrounds were eliminated by making cuts on the scatter plots of combinations of the following parameters: ΔE, time difference, position signals left and right of the proportional counter tube, and the energy signal in the solid state detector and in the ionization chamber.

The measured distributions of the total kinetic energies and the masses of the two fragments are shown in Figs. 1 and 2. In general the spectra have Gaussian shapes, as expected for high energy fission where shell effects are unimportant. The only exception is the mass distribution in the case of the silver target where the distribution shows more of a box-like form. Out of curiosity we have fitted a symmetric double Gaussian cumulative to the data and found that it gives a much better representation. This is also shown in Fig. 2.

*h.machner@fz-juelich.de

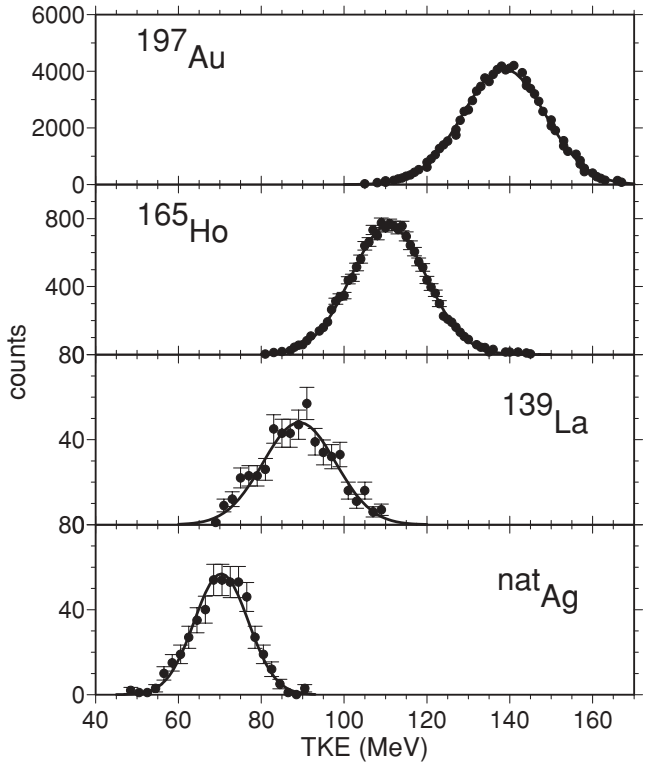

FIG. 1. Distributions of the total kinetic energy (TKE) for the four target nuclei studied. The data are shown as dots with error bars; fits with Gaussians are shown as solid curves.

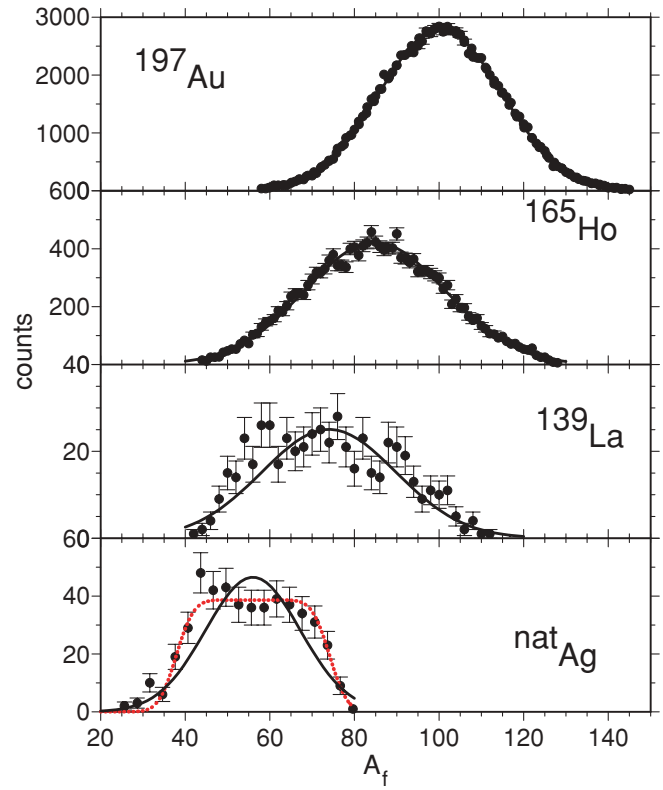

FIG. 2. (Color online) Same as Fig. 1 but for fragment masses. The fit with a symmetric double Gaussian cumulative in the case of Ag is shown as a dotted curve.

The measurements were so far analyzed assuming a fissioning system. These of course provide the most interesting information. However, the experiment records events after emission of particles before the fragments have reached the detectors. The best choice for a necessary correction would have been through the measurement of the corresponding particle spectra, but this was not done. However, we performed a measurement of the correlation angle between the two fission fragments in the case of the gold target and found an almost complete linear momentum transfer from the projectile to the fissioning system similar to that in Ref. [8]. Furthermore we calculated the mean momentum carried away near the forward direction by protons and neutrons during the pre-equilibrium phase by making use of the exciton model with standard input parameters [9]. In the case of the gold target, neutrons carry away ≈255 MeV/c but with 0.22 neutrons per incident α particle. For protons, the mean momentum is higher, ≈285 MeV/c, but the rate is only 0.14 protons per α particle. We, therefore, assume that the prefission neutrons are mainly emitted isotropically.

The average number of prefission neutrons $\nu_{\rm pre}$ was calculated with the ALICE code [10]. Here we employed ratios for the level density parameters a_f/a_n varying between 1.03 in the case of the gold target and 1.1 for silver. We tested this method by studying the compound nucleus ^{208}Po by using the results of Cuninghame *et al.* [11] who measured the total number of emitted neutrons from ^{208}Po by radiochemical methods. They then calculated the number of prefission neutrons with the ALICE code and extracted the average number of post-fission neutrons. The latter are emitted from the excited fragments as s waves and thus do not on the average change the fragment's velocity. Their results agree with the findings of Cheifetz *et al.* [12] who measured the prefission and the post-fission neutrons directly at some higher energies for ^{210}Po. It is interesting to note that the number of post-fission neutrons is only weakly energy dependent. The numbers for the energy and mass distributions, before and after corrections for neutron emission, are given in Table I.

In the following step, the influence of post-fission neutrons on the distributions is taken into account following the method of Ref. [13]. The resulting values are also given in Table I. Here we have corrected an overestimation of the pulse height defect in the case of the silver target, which is approximately 1 MeV.

Finally we performed one more comparison to test the procedure. Fission is treated in ALICE in the framework of the rotating liquid drop model [14]. We repeated the calculations for the case of the gold target with a combined cascade model code [15] and the statistical code GEM [16]. Contrary to the ALICE calculation, GEM, based on the RAL model [17], treats fission assuming empirical parametrizations. This limits fission to nuclei with $Z > 70$. The calculation gives a mean number of emitted neutrons of 11.1 which is a nice agreement to the sum 11.6 in Table I.

Viola and co-workers [18] found a remarkable correlation between the kinetic energy release and the Coulomb parameter $Z^2/A^{1/3}$ (Viola systematics). The corresponding values are

TABLE I. Widths and centroids with u the number of nucleons of the measured distributions for the different target nuclei. The average numbers of prefission neutrons $\langle\nu_{\rm pre}\rangle$ and post-fission neutrons $\langle\nu_{\rm post}\rangle$ as well as the quantities corrected for pre- and post-fission neutron emission are also given (indicated by an asterisk). The last row is the estimation of the mean total kinetic energy according to the Viola method [18].

Target	$^{\rm nat}$Ag	^{139}La	^{165}Ho	^{197}Au
σ_m (u)	11.2 ± 0.7	15.5 ± 0.8	16.6 ± 0.3	14.4 ± 0.1
$\langle$TKE$\rangle$ (MeV)	70.4 ± 0.3	89.2 ± 0.4	110.7 ± 0.1	138.6 ± 0.1
$\sigma_{\rm TKE}$ (MeV)	6.5 ± 0.2	8.8 ± 0.4	8.2 ± 0.1	10.0 ± 0.1
$\langle\nu_{\rm pre}\rangle$	1.0	1.5	2.7	7.0
$\langle\nu_{\rm post}\rangle$	5.6	6.2	6.6	4.1
σ_m^* (u)	10.2	15.0	16.2	13.8
$\langle$TKE$^*\rangle$ (MeV)	71.2	91.9	114.2	138.9
$\sigma_{\rm TKE}^*$ (MeV)	8.0	10.1	9.6	11.3
$\langle$TKE$\rangle_V$	66.6	86.4	109.7	140.7

also given in the table. The present values are slightly larger than those predicted by the systematics except for the case of gold.

We converted the measured count rates into cross sections by making use of the target thicknesses and the incident flux. The results are given in Table II.

In Fig. 3 our results are compared with other data. Also shown are calculations for nearby targets which describe remarkably well the experimental fission cross sections at lower energies. Our present data fill a gap between these lower energy data and results at higher energies [20]. It is worth noting that the cross section in the case of the lanthanum target is the smallest.

Another comparison is made on the basis of the fission probability as a function of the fissility parameter Z^2/A (see Fig. 4). The only data for 140 MeV α particles are for bismuth and uranium [21]. The fission probability for bismuth is almost an order of magnitude larger than that for gold and for uranium it is about unity. Since no data exist for α-particle induced fission for lower masses, we compare the present data with those from proton-induced reactions at energies close by. There is a remarkable agreement between the results for the two entrance channels, the minimum in the vicinity of $Z^2/A = 24$ is especially visible in both reactions. The fission probability

TABLE II. Cross section for fission for the different target nuclei. Also given are estimates for the fission barriers obtained by the linear dependence of the fission parameter [denoted by (I)] and on the exponential given in the text [denoted by (II)].

Target	$\sigma_{\rm fiss}$ (mb)	B_f (MeV) (I)	B_f (MeV) (II)
$^{\rm nat}$Ag	0.030 ± 0.007	38.8	49.1
^{139}La	0.007 ± 0.001	49.5	62.8
^{165}Ho	0.600 ± 0.050	40.8	45.4
^{197}Au	128 ± 18	26.9	25.7

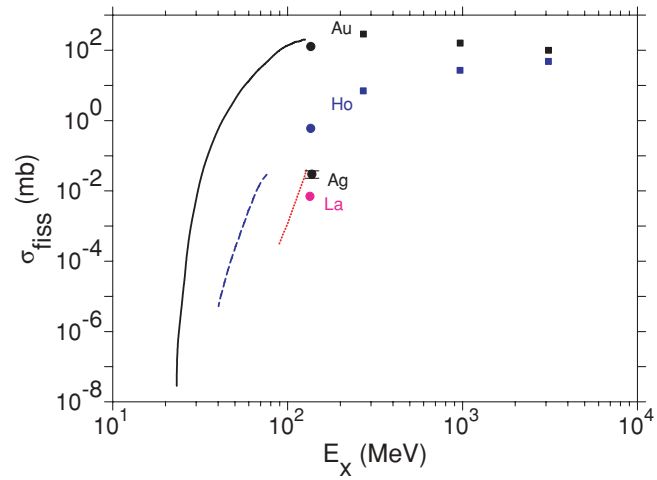

FIG. 3. (Color online) Excitation function for α-particle induced fission. The present data are shown as full dots with error bars with the target nucleus being indicated. The curves are calculations from Moretto [19] for In (dotted), Tm (dashed), and Au (solid). The results from Ref. [20] for Au and Ho are shown by crossed circles.

shows exponential dependencies: one slope for $24 \leqslant Z^2/A \leqslant 33$ and another one for $34.5 \leqslant Z^2/A$.

Obviously the variation of the fission probability reflects a variation of the fission barrier. In order to obtain a rough estimate we have extrapolated the Thomas-Fermi approach [27] to lower fissility parameters X, which depends not only on Z^2/A but also on the symmetry energy. For a range $30 \leqslant X \leqslant 34.14$ the original work found a linear relation of the reduced fission barrier $F(X)$ from fits to experiments. We have assumed this dependence to be valid also for smaller X. Alternatively

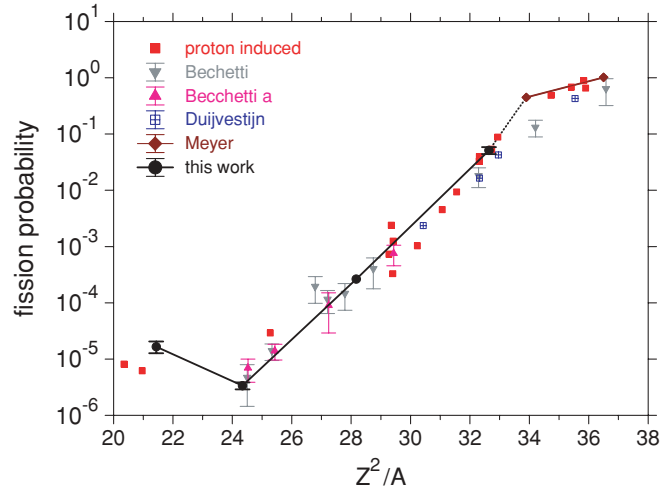

FIG. 4. (Color online) The fission probability as a function of the fissility parameter. The dots with error bars are the present results and diamonds are from Ref. [21]. The lines are to guide the eye. The squares are for proton-induced fission at energies 150 to 200 MeV [22,23]. The other data shown were measured with 190 MeV protons: triangles down [24], triangles up [25], and those shown by crossed squares were measured by radiochemical methods [26].

we have fitted functions to all available experimental data and found $F(X) = \exp(1.6248 - 5.504E - 05 * X^3)$. The barrier is then $B_f(A, Z) = S(A, Z) * F(X)$ with $S(A, Z)$ approximately the nominal surface energy of a nucleus. The results with both methods are also given in Table II. While the two methods give similar results in case of the gold target they diverge more for the lighter systems. However, both methods give a maximum for the lanthanum target which corresponds to minimum fission probability.

In summary, we have measured the binary fission of four nuclei from silver to gold induced by 140 MeV α particles. The distributions obtained for fragment masses and total kinetic energies were corrected for pre- and post-fission neutron emission. The mean values of the total kinetic energies are close to those predicted by the Viola systematics. The present data fill a gap or extend smoothly fission yields to higher energies. The measured fission probabilities show a distinctly different behavior from those observed for very heavy nuclei. This is in agreement with fission studies of proton-induced reactions at slightly higher beam energies. The increase in the relative width of the mass distribution from lanthanum on, as predicted by Ref. [28] on the basis of the liquid drop model, is not seen here. However, σ_m^*/A_{CN} decreases from lanthanum to silver.

The minimum of the fission probability around $Z^2/A = 20$ predicted by calculations within the liquid drop model [5] and in a more refined model [29,30] is not seen here but a minimum in the vicinity of $Z^2/A = 24$. This is in agreement with proton induced fission at energies close by and in photofission [31,32]. A crude estimate of fission barriers in a Thomas-Fermi approach yields a maximum for that value. The fragment mass distribution in the case of the silver target shows an almost rectangular shape while the other mass distributions look Gaussian. Such a behavior was found in fission of ^{232}Th with 190 MeV protons [26]. A possible explanation is that after neutron emission the low excited system still undergoes fission which is then asymmetric. This was also found in antiproton annihilation on ^{238}U [33]. However, such an explanation is very unlikely for silver-like compound nuclei. Therefore this case needs further investigation.

[1] R. Vandenboosch and J. R. Huizenga, *Nuclear Fission* (Academic Press, New York/London, 1973).
[2] C. Wagemans, *The Nuclear Fission Process* (CRC Press, Boca Raton, 1991).
[3] W. von Oertzen *et al.*, Phys. Rev. C **78**, 044615 (2008).
[4] U. L. Businaro and S. Gallone, Nuovo Cimento **5**, 315 (1957).
[5] J. R. Nix and E. Sassi, Nucl. Phys. **81**, 61 (1966).
[6] H. W. Schmitt, W. E. Kiker, and C. W. Williams, Phys. Rev. **137**, B837 (1965).
[7] B. Kaufmann *et al.*, Nucl. Instrum. Methods **115**, 47 (1974).
[8] V. E. Viola, C. T. Roche, W. G. Meyer, and R. G. Clark, Phys. Rev. C **10**, 2416 (1974).
[9] H. Machner, Phys. Rep. **127**, 309 (1985).
[10] M. Blann, Technical Report, LLNL Report No. UCRL-JC-, Lawrence Livermore National Laboratory (1991).
[11] J. G. Cuninhame *et al.*, *Physics and Chemistry of Fission 1979* (International Atomic Energy Agency, Vienna, 1980), Vol. I, p. 551.
[12] E. Cheifetz, Z. Fraenkel, J. Galin, M. Lefort, J. Péter, and X. Tarrago, Phys. Rev. C **2**, 256 (1970).
[13] F. Plasil *et al.*, Phys. Rev. **142**, 696 (1966).
[14] S. Cohen, F. Plasil, and W. J. Swiatecki, Ann. Phys. (NY) **82**, 557 (1974).
[15] J. Cugnon, C. Volant, and S. Vuillier, Nucl. Phys. **A620**, 475 (1997).
[16] S. Furihata, Nucl. Instrum. Methods Phys. Res. B **171**, 251 (2000).
[17] F. Atchison, "A Treatment of Fission for HETC," in *Intermediate Energy Nuclear Data: Models and Codes, Proceedings of a Specialists Meeting*, May 30–June 1, 1994, Issy-Les-Moulineaux, France (OECD, Paris, France, 1994), pp. 199–218.
[18] V. E. Viola, K. Kwiatkowski, and M. Walker, Phys. Rev. C **31**, 1550 (1985).
[19] L. G. Moretto, *Physics and Chemistry of Fission 1973* (International Atomic Energy Agency, Vienna, 1974), Vol. I, p. 329.
[20] G. Klotz-Engmann *et al.*, Nucl. Phys. **A499**, 392 (1989).
[21] W. G. Meyer, V. E. Viola, R. G. Clark, S. M. Read, and R. B. Theus, Phys. Rev. C **20**, 1716 (1979).
[22] V. S. Barashenkov and V. D. Toneev, *Interaction of High Energy Particles and Nuclei with Nuclei* (Atomizdat, Moscow, 1972), p. 566.
[23] O. E. Shigaev *et al.*, Radium Institut Leningrad report RI-17 (1973).
[24] F. D. Becchetti, J. Jänecke, P. Lister, K. Kwiatkowski, H. Karwowski, and S. Zhou, Phys. Rev. C **28**, 276 (1983).
[25] F. D. Becchetti, P. Lister, J. Jänecke, A. Nadasen, K. Kwiatkowski, H. Karwowski, and K. Hicks, Bull. Am. Phys. Soc. **28**, 698 (1983).
[26] M. C. Duijvestijn *et al.*, Phys. Rev. C **59**, 776 (1999).
[27] W. D. Myers and W. J. Swiątecki, Phys. Rev. C **60**, 014606 (1999).
[28] J. R. Nix, Nucl. Phys. **A130**, 241 (1969).
[29] A. S. Iljinov, E. A. Cherepanov, and S. E. Chigrinov, Z. Phys. A **287**, 37 (1978).
[30] D. I. Ivanov *et al.*, Z. Phys. A **352**, 191 (1995).
[31] T. Methasiri and S. A. E. Johansson, Nucl. Phys. **A167**, 97 (1971).
[32] V. Emma, S. Lo Nigro, and C. Milone, Nucl. Phys. **A257**, 438 (1976).
[33] H. Machner *et al.*, Z. Phys. A **343**, 73 (1992).